

Supporting Information

Super Tough and Self-healable Poly(dimethylsiloxane) Elastomer via Hydrogen

Bonding Association and its Applications as Triboelectric Nanogenerator

*Haiming Chen¹, J. Justin Koh^{1,2}, Mengmeng Liu¹, Pengju Li¹, Xiaotong Fan¹, Siqu Liu¹, Jayven C.C. Yeo¹, Yujun Tan^{1,3}, Benjamin C. K. Tee^{1,3,4,5}, Chaobin He^{*1,4}*

1. Department of Materials Science and Engineering, National University of Singapore, 9 Engineering Drive 1, Singapore 117575
2. Singapore Institute of Manufacturing Technology, Agency for Science, Technology and Research (A*STAR), 73 Nanyang Drive, Singapore 637662
3. Institute for Health Innovation & Technology (iHealthTech), National University of Singapore, 14 Medical Drive, Singapore, 117599, Singapore
4. Institute of Materials Research and Engineering, Agency for Science, Technology, and Research (A*STAR), 2 Fusionopolis Way, Innovis, Singapore 138634
5. Department of Electrical and Computer Engineering (ECE), National University of Singapore, Singapore, 117583

*Address correspondence to: msehc@nus.edu.sg

Table of content

Experimental section

Supporting figures and tables

Captions of Video S1 and S2

Supporting references

Experimental Section

Materials

Bis(3-aminopropyl) terminated poly(dimethylsiloxane) ($M_n=2500$, A-PDMS), bis(hydroxyalkyl) terminated poly(dimethylsiloxane) ($M_n=5600$, H-PDMS), 4,4'-methylenebis(cyclohexyl isocyanate) (HMDI), 2-acrylamido-2-methyl-1-propanesulfonic acid (AMPS), 2-amino-4-hydroxy-6-methylpyrimidine (UPy), sodium hydroxide solution (NaOH), ammonium persulfate (APS, 98%), hydrochloric acid (HCl, 37%) and acrylamide (AAm) were purchased from Sigma-Aldrich. Anhydrous tetrahydrofuran (THF) and methanol (MeOH) were purchased from Acros Organics. Dibutyltin dilaurate (DBTDL) catalyst was purchased from Alfa Aesar. All reagents were commercially available and used as supplied without further purification.

Synthesis of A_x-H_{10-x} series elastomers

First, A-PDMS and H-PDMS were mixed at a preset ratio and filled into a three-necked flask. The polymer mixture was then heated to 60 °C and stirred for 2 hours under vacuum condition for degassing and water removal purposes. Next, anhydrous THF (30 mL), DBTDL (10 μ L) and HMDI (0.98 mL) were added dropwise into the reaction flask, the reaction takes place under nitrogen atmosphere for 3 days. After the reaction, the solution was poured into MeOH (160 mL) and stirred for 30 minutes for the complete removal of residual HMDI as well as the catalyst. Subsequently, white precipitate-like viscous liquid appeared and the mixture was left to stand for 90 minutes, before filtering out the products and dissolving them in 40 mL THF. The dissolution-precipitation decantation process was repeated for three times and the final product was dried under vacuum conditions to remove residual solvent. All of the samples were named A_x-H_{10-x} depending on the mole ratio of A-PDMS and H-PDMS. For example, A_6-H_4 means the mole ratio of A-PDMS : H-PDMS is 6 : 4. The composition details can be found in **Table S1**.

The molecular weights and chemical structures of all A_x-H_{10-x} copolymer are as follows:

A₁₀-H₀: Molecular weight according to GPC: $M_w=26,700$; $M_n=18,600$ ($\bar{D} = 1.44$)
¹H NMR (500 M, CDCl₃): δ 7.46 (s, 1H), 7.38 (s, 1H), 7.27 (s, 4H), 7.05 (s, 1H), 6.98 (s, 1H), 3.77 (s, 4H).

A₈-H₂: Molecular weight according to GPC: $M_w=61,700$; $M_n=46,100$ ($\bar{D} = 1.34$)
¹H NMR (500 M, CDCl₃): δ 7.46 (s, 1H), 7.38 (s, 1H), 7.29 (s, 1H), 7.23 (s, 1H), 7.05 (s, 1H), 6.98 (s, 1H), 3.77 (s, 4H).

A₇-H₃: Molecular weight according to GPC: $M_w=82,000$; $M_n=58,100$ ($\bar{D} = 1.41$)
¹H NMR (500 M, CDCl₃): δ 7.47 (s, 1H), 7.38 (s, 1H), 7.29 (s, 1H), 7.23 (s, 1H), 7.05 (s, 1H), 6.98 (s, 1H), 3.77 (s, 4H).

A₆-H₄: Molecular weight according to GPC: $M_w=94,900$; $M_n=73,400$ ($\bar{D} = 1.29$)
¹H NMR (500 M, CDCl₃): δ 7.47 (s, 1H), 7.38 (s, 1H), 7.29 (s, 1H), 7.23 (s, 1H), 7.05 (s, 1H), 6.98 (s, 1H), 3.77 (s, 4H).

A₅-H₅: Molecular weight according to GPC: $M_w=97,900$; $M_n=79,000$ ($\bar{D} = 1.24$)
¹H NMR (500 M, CDCl₃): δ 7.47 (s, 1H), 7.38 (s, 1H), 7.29 (s, 1H), 7.23 (s, 1H), 7.05 (s, 1H), 6.98 (s, 1H), 3.77 (s, 4H).

Fabrication of A_x-H_{10-x} elastic films

The above prepared solid samples were re-dissolved in THF solvent at a concentration of 0.2 g/mL, before casting on Teflon dish. After the solvent evaporated, the samples were vacuum dried at room temperature for 24 hours to ensure total removal of residual solvent. Finally, the obtained films were cut into rectangular shapes with the size of 15 mm \times 10 mm \times 0.5 mm (length \times width \times thickness) by a razor blade. For the colored specimen, small amount of red, grey and blue dyes were dripped into the THF solution, respectively, followed by the exact same procedure as mentioned above.

Synthesis of 2-(6-isocyanato-cyclohexylamino)-6-methyl-4[1H]-pyrimidone

The synthesis of 2-(6-isocyanato-cyclohexylamino)-6-methyl-4[1H]-pyrimidone was performed according to a literature¹. In detail, 2-Amino-4-hydroxy-6-methylpyrimidine (16 mmol, 2.00 g) was mixed with 5 equiv of HMDI (80 mmol, 20.96

g). The mixture was put in a round bottom flask and stirred at 100 °C for 24 h under N₂ atmosphere. The reaction mixture was extensively washed by hexane to remove the unreacted HMDI. The product was dried at 60 °C under vacuum overnight to obtain white powder (5.64 g, yield, 91%). The NMR result is shown in **Figure S15**.

Synthesis of acrylamide terminated UPy unit

The above synthesized 2-(6-isocyanato-cyclohexylamino)-6-methyl-4[1H]-pyrimidone (10 mmol, 3.87 g) was mixed 5 equiv of AAm (50 mmol, 3.6 g). The mixture was put in a round bottom flask and stirred at 100 °C for 24 h under N₂ atmosphere. The reaction mixture was extensively washed by deionized water to remove the unreacted AAm. The product was dried at 60 °C under vacuum overnight to obtain white powder (4.31 g, yield, 94%). The NMR result is shown in **Figure S16**.

Synthesis of PAMPS-U10

The PAMPS-U10 based on AMPS with 10 % mole ratio acrylamide terminated UPy unit were prepared by one-pot free radical polymerization. AMPS (9 mmol, 1.86 g), acrylamide terminated UPy unit (1 mmol, 0.46 g) and APS (0.01 mmol, 2.3 mg) were dissolved in aqueous solution (30 w/v%) and the pH of the solution was adjusted to 13 by NaOH to facilitate the dissolution of acrylamide terminated UPy unit. Then the polymerization was conducted at 70 °C for 6 h in a sealed vial, yielding a viscous solution for use.

Fabricating of single-electrode triboelectric nanogenerator (s-TENG) device

First, A₆-H₄ elastic film with same size 50 mm × 50 mm × 0.25 mm (length × width × thickness) were prepared. Then, the above PAMPS-U10 aqueous solution (30 w/v%) was injecting by syringe onto the A₆-H₄ elastic film and controlling the area is about 40 mm × 15 mm (length × width), which is smaller than the A₆-H₄ elastic film. After the PAMPS-U10 layer reaching up to an equilibrium state by water evaporating for three days, one piece of aluminum foil was attached onto PAMPS-U10 layer. Then the A₆-H₄ elastic film was folded by one side to other side and make sure the closely contact

of two A₆-H₄ faces. After more three days self-healing of A₆-H₄ film, the s-TENG with sandwich structure was obtained.

Characterisation

Analytical gel permeation chromatography (GPC) experiments were performed on a Malvern VE2001 GPC solvent/sample Module with three ViscoGEL™ I-MBHMW-3078 columns. HPLC grade THF was used as eluent at a flow rate of 1.0 mL/min. Monodispersed poly(methyl methacrylate) standards were used to obtain a calibration curve. ¹H Nuclear Magnetic Resonance (¹H-NMR) spectra were measured by JEOL 500 MHz spectrometer using CDCl₃ as a solvent at room temperature. *In-situ* Fourier Transform Infrared (FTIR) spectra were measured using a Nicolet 6700 spectrometer equipped with Linkam TST 350 hot stage and a DTGs detector by averaging 32 scans at a 4 cm⁻¹ resolution, the film was heated from -50 °C to 100 °C with a heating rate of 3 °C/min. Absorption spectra were measured by a Shimadzu UV-1800 spectrophotometer, the background was normalized first by two blank glass slides. Then the samples were attached onto one glass slide for measuring, and another glass slide was used as reference. Thermogravimetric Analyzer (TGA) experiments were carried out with a TA instruments' TGA Q500 with a heating rate of 20 °C/min from 50 to 700 °C. Dynamic mechanical analysis (DMA) was carried out on specimens cut from solution-cast films with a TA instruments' DMA Q800 uniaxial tension mode at a temperature range of -100 to 120 °C with a heating rate of 3 °C/min, oscillation frequency of 1 Hz and oscillation strain of 1%. Small angle X-ray scattering (SAXS) were measured by Xeuss 2.0 SAXS/WAXS system (Xenocs SA, France). Cu Kα X-ray source (GeniX3D Cu ULD), generated at 50 kV and 0.6 mA, was utilized to produce X-ray radiation with a wavelength of 1.5418 Å. A semiconductor detector (Pilatus 200 K, DECTRIS, Swiss) with a resolution of 487 × 619 pixels (pixel size = 172 × 172 μm²) was used to collect the scattering signals. Each SAXS pattern was collected with an exposure time of 60 min. The one-dimensional intensity profiles were integrated from background corrected 2D SAXS patterns. The water contact angles (WCA) were measured using a video contact angle system (VCA Optima) under ambient conditions.

Static contact angles were obtained by averaging the values measured from 5 μL of deionized water droplets of five independent tests. Mechanical properties conducted at room temperature by using an Instron 4505 tensile machine with a specific crosshead speed illustrated in paper. Five specimens of each composition were tested, the data reported were the average values. Polarized Optical Microscopy (POM) images were taken using Nikon ECLIPSE LV100. The samples were notched before stretching and subsequently stretched to 100 % strain and fixed on the glass slides. Scanning electron microscopy (SEM) images were obtained with a field-emission scanning electron microscope (Zeiss Supra 40 FE-SEM) at an operating voltage of 5 kV. Atomic force microscope (AFM, Bruker) was carried out to measure the morphology with tapping mode. The electrical conductivity was measured by a sourcemeter (Keithley 2450). The output voltage were recorded by KEYSIGHT MSOX2024A Mixed Signal Oscilloscope. A step motor (Newmark linear stage/Mark-10 system) with force of 5 N, round contact area of 1 cm^2 was used to provide the input of mechanical motions.

Supporting figures and tables

Table S1. Elastomers name and their chemical composition details.

Samples	Mole ratio		volume (mL)			
	A-PDMS	H-PDMS	A-PDMS	H-PDMS	HMDI	DBTDL
A ₁₀ -H ₀	10	0	10.310	---	0.98	0.01
A ₈ -H ₂	8	2	8.248	4.572	0.98	0.01
A ₇ -H ₃	7	3	7.220	6.856	0.98	0.01
A ₆ -H ₄	6	4	6.186	9.142	0.98	0.01
A ₅ -H ₅	5	5	5.156	11.428	0.98	0.01

Table S2. The mechanical properties of A_x-H_{10-x} elastomers, at tensile rate of 10 min⁻¹.

Samples	Modulus (MPa)	Strength (MPa)	Elongation at break (%)	Toughness (MPa)
A ₁₀ -H ₀	7.31 ± 0.61	3.55 ± 0.48	610 ± 78	16.59 ± 0.99
A ₈ -H ₂	1.89 ± 0.27	2.19 ± 0.27	1160 ± 120	16.18 ± 0.87
A ₇ -H ₃	1.03 ± 0.23	2.17 ± 0.19	2214 ± 107	25.62 ± 1.42
A ₆ -H ₄	0.75 ± 0.14	0.98 ± 0.13	2334 ± 89	12.67 ± 0.56
A ₅ -H ₅	0.32 ± 0.09	0.43 ± 0.05	2326 ± 110	6.4 ± 0.32

Table S3. The mechanical properties of A₆-H₄ polymer under different tensile rates.

Tensile rate (min ⁻¹)	Modulus (MPa)	Strength (MPa)	Elongation at break (%)	Toughness (MPa)
2	0.31 ± 0.08	0.59 ± 0.09	3135 ± 107	11.48 ± 0.37
4	0.45 ± 0.11	0.72 ± 0.12	2641 ± 97	11.46 ± 0.42
10	0.75 ± 0.14	0.98 ± 0.13	2334 ± 89	12.67 ± 0.56
20	0.77 ± 0.20	1.19 ± 0.18	2001 ± 79	13.44 ± 0.51
40	0.87 ± 0.21	1.27 ± 0.26	1873 ± 81	13.57 ± 0.39

Table S4. The fitted stress relaxation parameters of A₇-H₃ film based on the Maxwell model.

Strain (%)	S ₀	S ₁	S ₂	S ₃	T ₁ (sec)	T ₂ (sec)	T ₃ (sec)
200	0.0626	0.378	0.134	0.116	8.39	76.5	728
500	0.123	1.24	0.256	0.228	7.26	76.8	671
1000	0.185	3.98	0.466	0.383	6.55	82.6	788

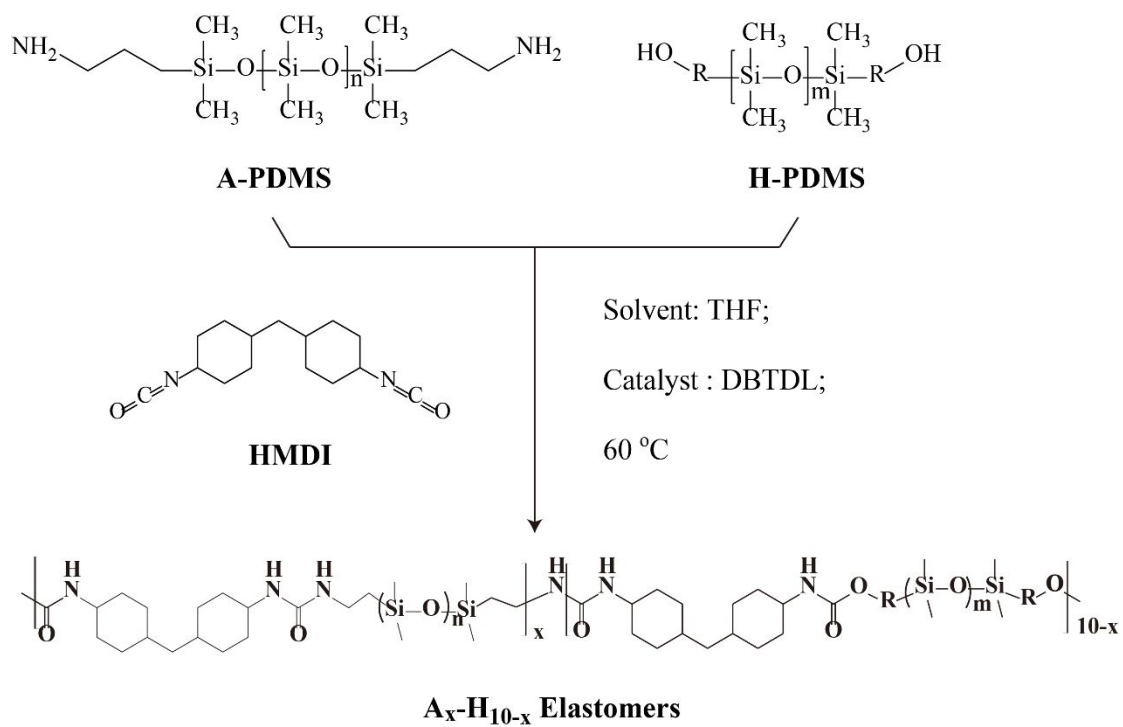


Figure S1. Synthetic route of A_x-H_{10-x} series elastomers.

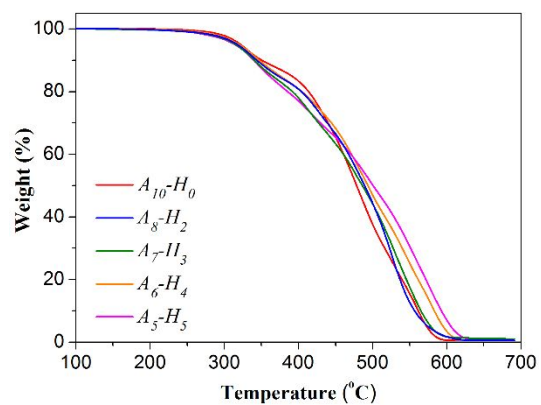


Figure S2. Thermogravimetric curves of A_x-H_{10-x} series elastomers.

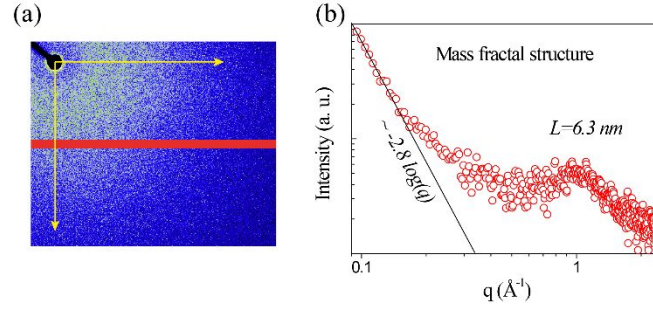


Figure S3. The 2D SAXS pattern (a) and 1D SAXS curve (b) of A₆-H₄ film. After correcting the background, the curve shows the relationship of $\text{Log}(I) \sim -2.8 \text{ Log}(q)$. According to Porod's law ($\text{Log}(I) \sim -D \text{ Log}(q)$), if $D < 3$, means the object belong to mass fractal structure.

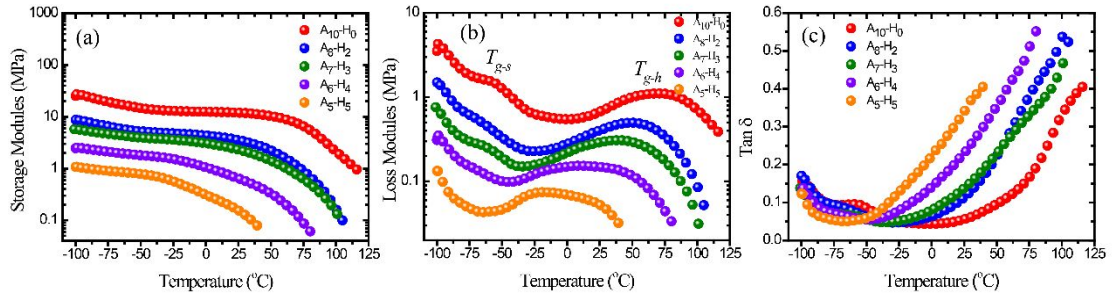


Figure S4. (a) The storage modules, (b) loss modulus and (c) $\tan \delta$ of A_x-H_{10-x} elastomers, respectively. More strong hydrogen bondings was introduced with increasing of the shorter chains length A-PDMS, resulting in the increase of storage modules and glass transition temperatures of the material.

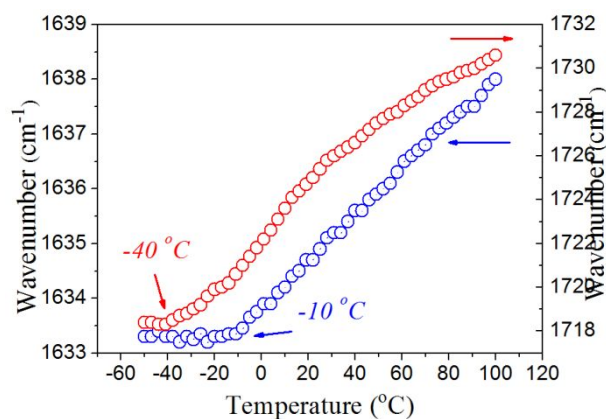


Figure S5. The location tracking curves of the ordered H-bond of C=O in urea group (blue) and the H-bond of C=O in urethane group (red) in A₆-H₄ elastic film. The blue-shifts indicate the weakening of the hydrogen bonding, which starts from -40 °C and -10 °C for the H-bonding of C=O in urethane group and the ordered H-bonding of C=O in urea group, respectively.

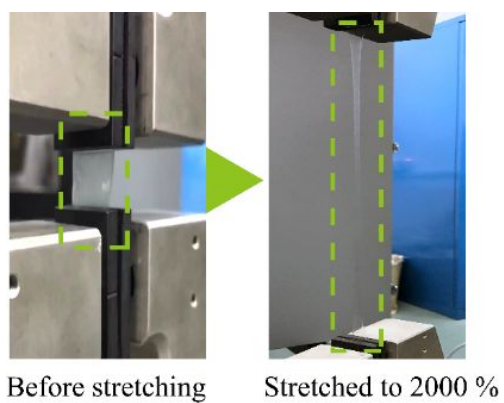


Figure S6. Optical images of A₆-H₄ film before stretching and after being stretched to 2000 % strain at a deformation speed of 10 min⁻¹ without rupturing, indicating extremely high stretchability.

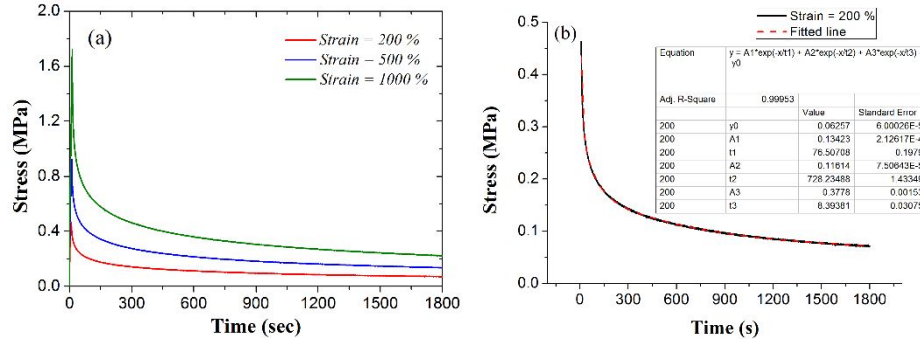


Figure S7. (a) Stress-relaxation behaviors of A₇-H₃ film subjected to different stretch ratios. Similar stress relaxation behaviors were observed in all tests despite the large variation in the stretch ratio. The larger stretch ratio results in a larger residual stress even after long time periods. (b) The 200 % strain A₇-H₃ film stress relaxation curve and curve fitted line by using a generalized Maxwell model with three exponential terms $S = S_0 + \sum_{i=0}^3 S_i \exp(-\frac{t}{T_i})$, where S and S_0 are immediate stress and original stress, respectively, T_i is the relaxation time.

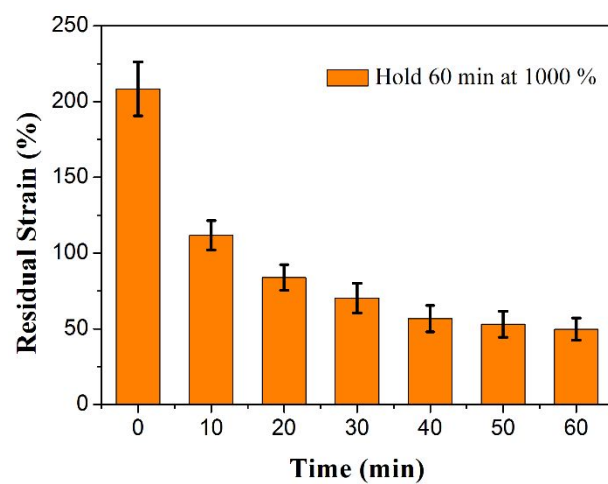


Figure S8. Residual strain with respect to the holding time of up to 60 min of the A₆-H₄ film as it relaxes after stretching to 1000 % strain.

Determination of fracture energy

The fracture energy (Γ) was determined by using a method introduced by Rivlin and Thomas². For each material composition, two samples of the same size were required, one notched and one unnotched. The unnotched sample was stretched to measure the force-length curve. When the two clamps were pulled to a distance L , the area beneath the force-length curve represents the work done by the applied force, $U(L)$. The notched sample was prepared by cutting the elastomers with a notch of length 4~5 mm using a razor blade. It is also noteworthy that the precise length of the notch is insignificant for this test.³ The notched sample was stretched until the notch turned into a running crack. The fracture energy can be calculated from:

$$\Gamma = \frac{U(L_c)}{a_0 b_0} \quad \text{Equation S1}$$

Where a_0 and b_0 is the width and thickness of the samples, respectively; L_c is the rupturing critical distance.

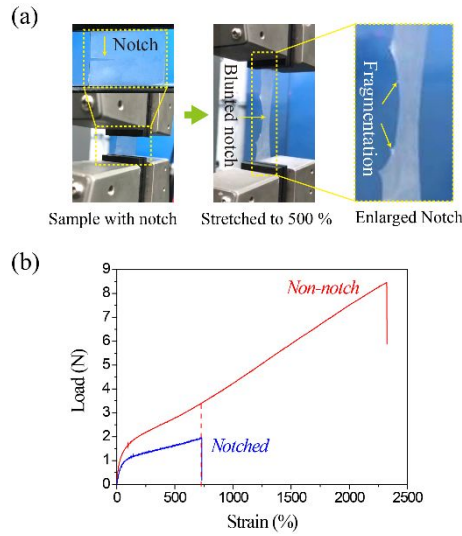


Figure S9. (a) The optical photos A₆-H₄ notched specimen before and after stretching to strain at 500 % and (b) Load-strain curves of A₆-H₄ notched and unnotched specimen.

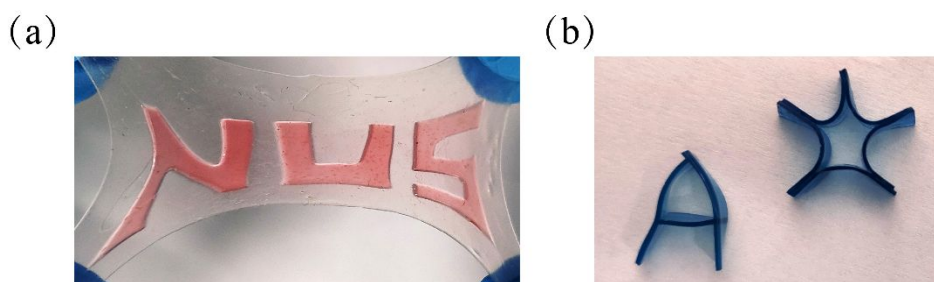


Figure S10. Solid welding experiments of A_6-H_4 film. (a) Three small pieces of red dye-stained A_6-H_4 film in the shape of “NUS” were left on top of a larger rectangular piece of A_6-H_4 film substrate to allow joining to take place at room temperature for 72 hours with a gently applied pressure. The resulting inscribed film is biaxially stretched without any delamination taking place, suggesting a good adhesion at the interface. (b) Eight pieces of blue dye-stained A_6-H_4 film were welded into two different 3D structures at room temperature for 72 hours. Suggesting that the material can be processed into complex 3D structures in similar fashion, such as a letter “A” and a pentagram, simply by joining few pieces together.

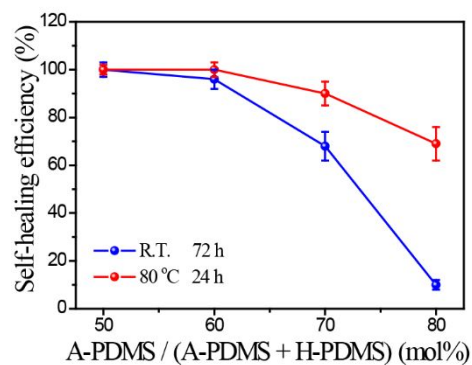


Figure S11. Self-healing efficiency of the A_x-H_{10-x} elastomers ($x=5, 6, 7, 8$) at different conditions as a function of mole ratio of A-PDMS. The self-efficiency is calculated based on the ratio of the elongation at break between the self-healed one and the original one. The formulas can be expressed as

$$\text{Self-healing efficiency } (\eta) = \frac{\text{Elongation at break of self-healed one}}{\text{Elongation at break of original one}} \times 100 \%$$

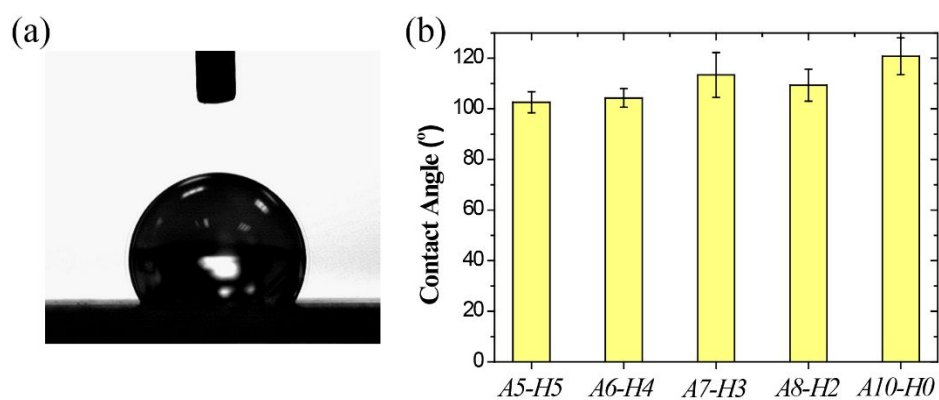


Figure S12. (a) Optical photo of water contact onto A₆-H₄ film. (b) Water contact angles of A_x-H_{10-x} elastomers.

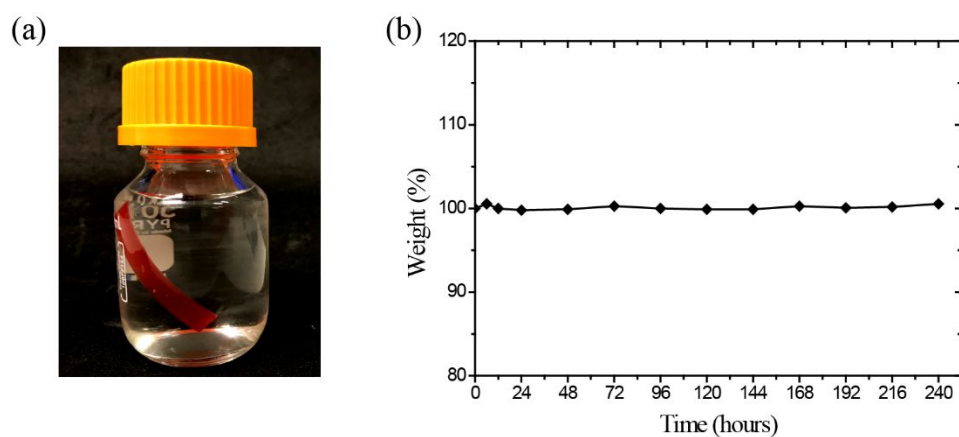


Figure S13. Water-proof property experiment of A₆-H₄ film. (a) Red dye-stained A₆-H₄ film soaked in water. (b) Weight variation of A₆-H₄ film after being soaked in water for different periods. The weight almost keeps invariant against the time, indicating no water-absorption when immersing polymer film into the water.

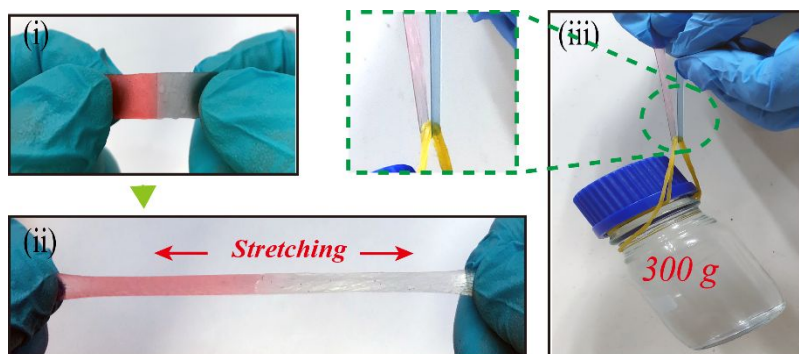


Figure S14. Underwater self-healing ability and stretchability of underwater self-healed A_6-H_4 film: (i) digital images of two different colored pieces A_6-H_4 film self-healed underwater for 72 hours. The self-healed film shows good (ii) stretchability and (iii) strength by lifting a 300 g bottle.

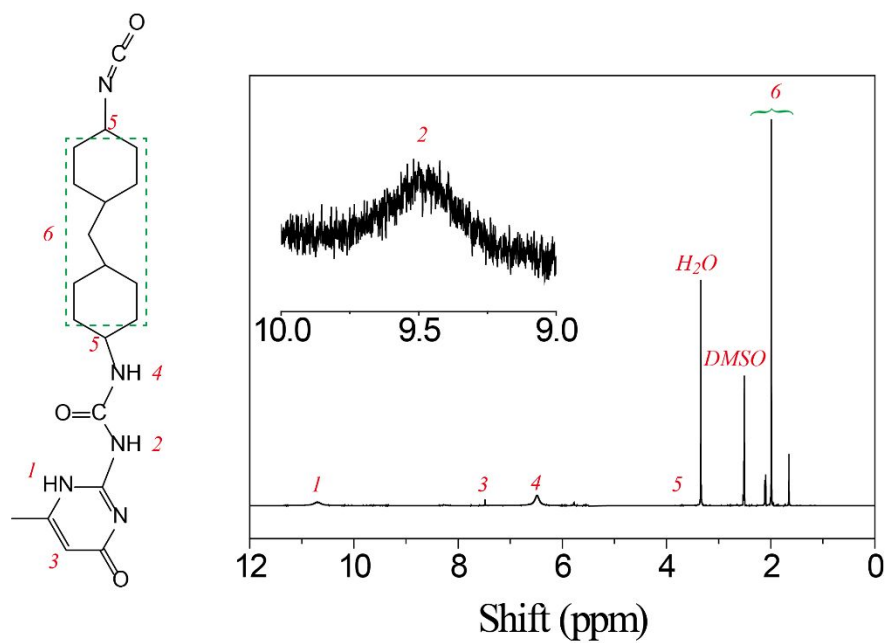


Figure S15. The chemical structure and NMR curve of 2-(6-isocyanato-cyclohexylamino)-6-methyl-4[1H]-pyrimidone.

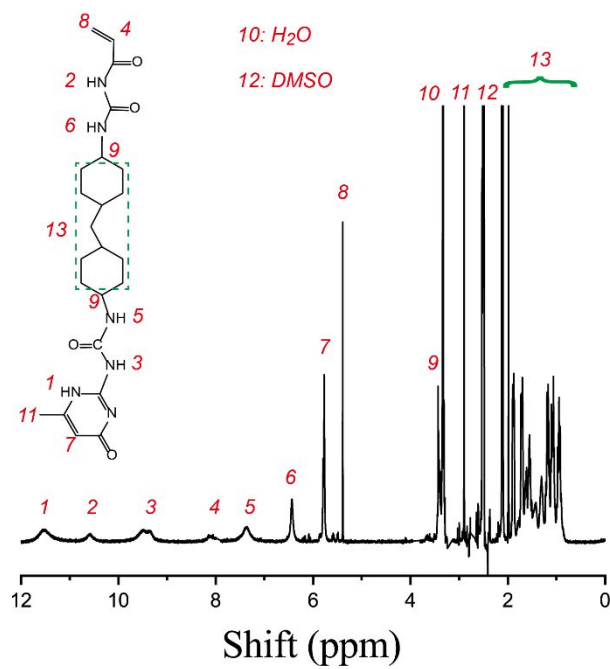


Figure S16. The chemical structure and NMR curve of acrylamide terminated UPy unit.

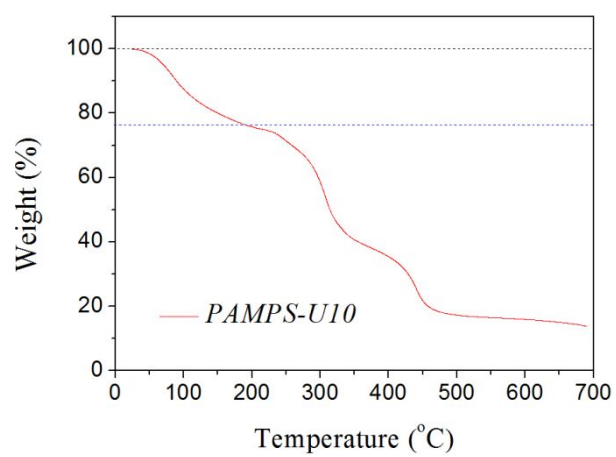


Figure S17. TGA curve of PAMPS-U10 polymer.

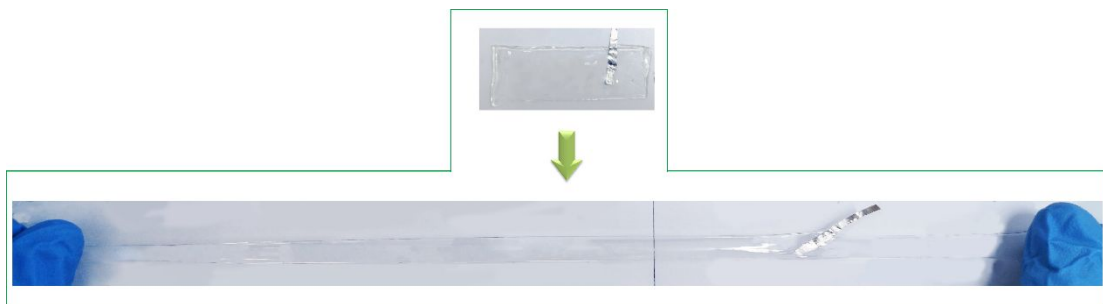


Figure S18. The optical image of s-TENG can be stretched by hand to 8 times the original length.

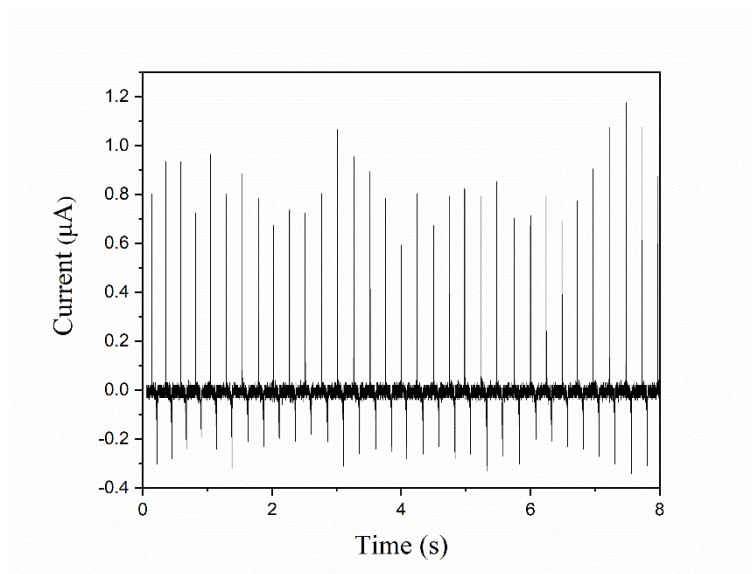


Figure S19. Current of s-TENG under the contact force of 5 N and contact area of 1 cm².

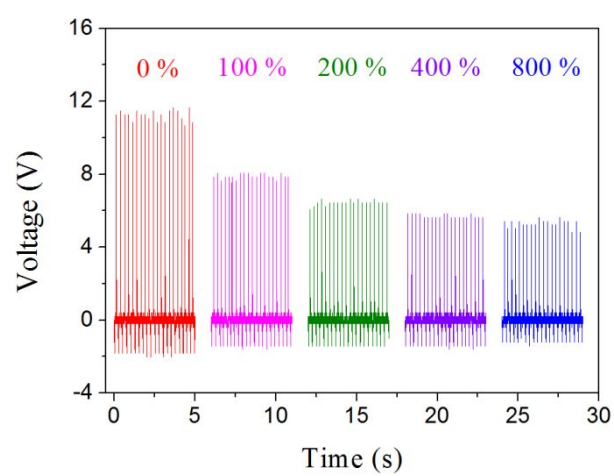


Figure S20. V_{OC} of s-TENG at different stretching ratio under the contact force of 5 N.

Video S1. The experiment of simply pressing to lighten up digital display.

Video S2. The experiment of peeling off s-TENG from digital display surface to lighten up digital display.

Supporting References:

1. Y. Song, Y. Liu, T. Qi and G. L. Li, *Angew.e Chem. Int.Ed.* 2018, **57**, 13838-13842.
2. R. S. Rivlin and A. G. Thomas, *J. Polym. Sci.* 1953, **10**, 291-318.
3. J.-Y. Sun, X. Zhao, W. R. K. Illeperuma, O. Chaudhuri, K. H. Oh, D. J. Mooney, J. J. Vlassak and Z. Suo, *Nature*, 2012, **489**, 133.